BUDAPEST UNIVERSITY OF TECHNOLOGY AND ECONOMICS
FACULTY OF TRANSPORT ENGINEERING

Elaboration of Condition of Rapid Prototyping to Selective Laser Sintering and Investigation of Fe-Ni-Cu(P) Based Models

Summary of Ph.D. thesis

Author:
Szabolcs HERCZEG
M.Sc.

Director of studies:
dr. János Takács
professor and head of department

Budapest
2006

[12] W. König, T. Celiker, Y.-A. Song: Process Development for Direct Manufacturing of Metallic Parts; Proceedings of the LANE'94, Vol. II., 1994 - pp.: 785 - 792., ISBN 3-87525-061-3
[13] H. H. Zhu, L. Lu, J. Y. H. Fuh: Development and characterisation of direct laser sintering Cu-based metal powder; Journal of Materials Processing Technology 140, 2003 - pp.: 314-317.
[14] B. ODonnchadha, A. Tansey: A note on rapid metal composite tooling by selective laser sintering; Journal of Materials Processing Technology 153-154, 2004 - pp.: 28 - 34.
[15] D. King, T. Tansey: Rapid tooling selective laser sintering injection tooling; Journal of Materials Pocessing Technology 132, 2003 - pp.: 42 - 48.
[16] G. Reinhart, M. Meindl, M. Carnevale: Indirect Metal Laser Sintering Supporting Pressure Die Casting; Proceeding of LANE 2001, Meisenbach Verlag, Bamberg 2001 - pp.: 341 - 352., ISBN 3-87525-154-7
[17] F. Miani, E. Kuljanic, M. Sortion: Modelling the Mechnical Properties of Direct Metal Selectively Laser Sintered Parts; Proceeding of LANE 2001, Meisenbach Verlag, Bamberg 2001 - pp.: 383 - 390., ISBN 3-87525-154-7
[18] F. Niebling, A. Otto, M. Geiger: FE-Simulation des selektiven Laserstrahlsinterns von Metallpulver; Laser Opto 32(6), 2000 - pp.: 68 - 71.
[19] M. Anton: LS Laser Sintern - Herstellungsverfahren für Metallische Prototypen; Rapid Prototyping and Tooling VDI-Berichte Nr. 1686, 2002 - pp.: 92-95., ISBN 3-18-091686-9
[20] G. Witt, T. Brei: Vom Metallpulver zum Gesenk / Bauteil; Rapid Prototyping and Tooling VDI-Berichte Nr. 1686, 2002 - pp.: 69-89., ISBN 3-18-091686-9
[21] C. Ader: Direktes Lasersintern keramischer Feingusskomponenten; Rapid Prototyping and Tooling VDI-Berichte Nr. 1686, 2002 - pp.: 57-67., ISBN 3-18-091686-9
[22] M. Meindl: Indirektes Metall-Lasersintern für den Einsatz im Rapid Manufacturing; Laser Opto 32(6), 2000 - pp.: 72 - 75.
[23] D. Nellessen: Rapid Technologies im Versuchsfahrzeugbau; Rapid Prototyping and Tooling VDI-Berichte Nr. 1686, 2002 - pp.: 3 - 16., ISBN 3-18-091686-9
[24] S. Apichartpattanasiri, J. N. Hay, S. N. Kukureka: A study of the tribological behaviour of polyamide 66 with varying injection-moulding parameters; Wear 251, 2001, pp.: 1557 - 1566.
[25] Valasek I.: Tribológiai kézikönyv; Tribotechnik Kft, Budapest 1996 , ISBN 963 02 98368
[26] H. Unal, U. Sen, A. Mimaroglu: Dry sliding wear characteristics of some industrial polymers against steel counterface; Tribology International 37, 2004 - pp.: 727 - 732.
[27] Y. K. Chen, O. P. Modi, A. S. Mhay, A. Chrysanthou, J. M. O'Sullivan: The effect of different metallic counterface materials and different surface treatments on the wear and friction of polyamide 66 and its composite in rolling-sliding contact; Wear 255, 2003, pp.: 714 - 721.
[28] Verband Deutscher Maschinen- und Anlagenbau (VDMA): Kenndaten für die Verarbeitung thermoplastischer Kunststoffe, Teil 3, Tribologie; Carl Hanser Verlag, München 1983 - p.: 530., ISBN 3-446-13062-4
[29] Z. Chen, T. Li, Y. Yang, X. Liu, R. Lv: Mechanical and tribological properties of PA/PPS blends; Wear 257, 2004, pp.: 696 - 707.
[30] J. Takács, L. Tóth, F. Franek, A. Pauschity, T. Sebestyén: Investigation of Tribological Properties of Laser-Sintered and Coated Parts, 2nd Word Tribology Congress, Vienna, September 3 - 7. 2001, ISBN 3-901657-08-8
[31] Kalácska G.: Műszaki műanyagok gépészeti alapjai; Minerva-Sop bt, Sopron 1997 - p.: 120., ISBN 963 04 8704 7
[32] Quadrant GmbH. on-line termékkatalógus, webhely: www.quadrantplastics.com
[33] J & A Plastics GmbH. on-line termékkatalógus, webhely: www.j-a.de
[34] Ensinger Ltd. on-line termékkatalógus, webhely: www.ensinger.ltd.uk

[S15] Sz. Herczeg, J. Takács, L. Tóth, F. Franek, A. Pauschitz, T. Sebestyén: Investigation of properties of rapid prototype tool elements produced by selective laser sintering, Proceedings of the 11th International Conference on Tools ICT-2004, Miskolc, september 9-11, 2004, pp. 271-276, ISSN 1215-0851

[S16] Sz. Herczeg, J. Takács, L. Tóth, F. Franek, A. Pauschitz, T. Sebestyén: Tribological analysis of Fe- Ni -Cu alloy produced by selective laser sintering, Laser Assisted Net Shape Engineering 4, Erlangen, september 21-24, 2004, pp. 535-544 in Volume 1, ISBN 3-87525-202-0

[S17] Keszte R., Herczeg Sz., Takács J.: Korszerű technológiák a felületei tulajdonságok alakításában, Gyors prototípus készítés fejezete, Műszaki Könyvkiadó, Budapest, 2004, p. 346, ISBN 963 420 789 8

[S18] Herczeg Sz.: Újdonságok a lézeres gyártás területén, Magyar Műszaki Magazin III. évf. 11. szám, 2004. november, pp. 44-45, ISSN 1588-9300

[S19] Takács J., Herczeg Sz.: Gyors prototípus-készítés, Gép Műszaki Folyóirat LV. évf. 12. szám, 2004. december, pp. 42-47, ISSN 0016-8572

[S20] Sz. Herczeg, J. Takács: Investigation of wearing surface of selective-laser-sintered rapid prototyping specimens, Proceedings of 22nd International Colloquium on Advanced Manufacturing and Repair Technologies in Vehicle Industry, Czestochowa, may 18-20, 2005, pp. 55-60., ISBN 80-8070-393-0

[S21] Herczeg Sz., Takács J.: Gyors szerszámgyártás a járműiparban, 36. Autóbusz Szakértői Tanácskozás Nemzetközi Gépjárműbiztonsági Konferencia, 2005. augusztus 29-31., CD-ROM, 5. szekció: Gyártás, technológia, ISBN 963219070-X

9. Bibliography

[1] F. Niebling, A. Otto: FE-Simulation of the Selective Laser Sintering Process of Metallic Powders; Proceeding of LANE 2001, Meisenbach Verlag, Bamberg 2001 - pp.: 371 - 382., ISBN 3-87525-154-7

[2] Ph. Clementz, J. N. Pernin: Homogenization modeling of capillary forces in selective laser sintering; International Journal of Engineering Science 41, 2003 - pp.: 2305 - 2333.

[3] J. P. Kruth, L. Froyen, J. Van Vaerenbergh, P. Mercelis, M. Rombouts, B. Lauwers: Selective laser melting of iron-based powder; Journal of Materials Processing Technology 149, 2004 - pp.: 616 - 622.

[4] M. L. Murphy, W. M. Steen, C. Lee: The Rapid Manufacture of Metallic Components by Laser Surface Cladding; Proceedings of the LANE'94, Vol. II., 1994 - pp.: 803 - 813., ISBN 3-87525-061-3

[5] O. Nyrhilä, J. Hänninen, J. Kotila, J.-E. Lind, T. Syvänen: The Effect of Layer Thickness in the Direct Metal Laser Sintering Process; Proceeding of LANE 2001, Meisenbach Verlag, Bamberg 2001 - pp.: 363 - 370., ISBN 3-87525-154-7

[6] R. Leibelt, R. Dierken, P. Hoffman: Laser Sintering of Iron Based Powders; European Conference on Laser Treatment of Materials, Hanover, September 22 - 23. 1998 - pp.: 431 - 436, ISBN 3-88355-263-1

[7] M. Shellabear, O. Nyrhilä: DMLS - Development History and State of the Art; Proceeding of LANE 2004, Meisenbach Verlag, Bamberg 2004 - pp.: 393 - 404, ISBN 3-87525-202-0

[8] T. Wohlers: State of the Industry and Technology Update, Proceedings of EuroMould 2003

[9] Szabó O.:Fejlődési trendek a mikrométer- és nanométer pontosságú gyártásban (Plenáris előadás / cikk); Fiatal Műszakiak Tudományos Ülésszaka IX.kötet, EME, Kolozsvár, 2004. pp. XVII-XXVIII.(12p.) ISBN 973-8231-2o-4

[10] Szabó Ottó:High Accuracy Machining and Technology of Form Surfaces; Production Process and Systems, A Publication of the University of Miskolc. Vol. 1 (2oo2), University Press, Miskolc, 2oo2. pp.223-228. HU ISSN 1215-0851

[11] D. Binder: New solution for the improvement of metallic prototypes regarding surface quality, dimensional changes and solidity; European Conference on Laser Treatment of Materials, Hanover, September 22 - 23. 1998 - pp.: 425 - 430, ISBN 3-88355-263-1

CONTENTS

1. Introduction 1

2. Aim of the research work 1

3. Materials, equipments and methods 2

3.1. Materials 2

3.2. Equipments of experiment 3

3.3. Equipments of investigations 4

4. Investigation of the laser sintered specimen 4

4.1. Process parameters of laser sintering 4

4.2. The effects and the limits of the laser scanning speed 5

5. Tribological investigations 9

5.1. Sliding distance dependence of friction coefficient 9

5.2. Friction coefficient depending on sliding velocity 10

5.3. Friction coefficient depending on loading force 12

5.4. Investigation of temperature during the wearing processes 14

6. Summary 15

7. Summary of the new scientific results in thesis 16

8. Publications 18

9. Bibliography 19

1. Introduction

From the available literature it is established that the selective laser sintering is a modern and special rapid prototyping process [1, 2, 3, 4, 5]. Rapid prototyping (RP) methods are developing quickly and there are millions of RP models produced worldwide [6, 7, 8, 9, 10].
A lot of parameters influence the laser sintered bond. Many of these have not been investigated yet therefore we can only infer the processes occurring during the laser sintering. Because of the insufficiencies we are able only to deduce the processes during the laser sintering process.
The laser sintered rapid prototyping model can be used for design purposes but also to create functional prototypes. For the demonstration model the geometrical properties are important, but at a functional prototype the focus is on the mechanical properties. In the literature there are data about the laser beam scanning speed, the layer thickness, the laser power etc., but there are no data about their optimisation for the mechanical properties.
The composition of a typical metal powder for selective laser sintering is a mixture of iron, nickel and phosphorous-bronze. But there are no data about technological parameters in the production and even less about the optimisation of these parameters. We can only infer these parameters from other investigations made with iron, copper or nickel [11, 12, 13, 14, 15].
If the rapid prototype model is used for functional testing then its duration becomes very important as well. The laser sintered workpieces are often built together with polymer components [5, 14, 15, 16, 17, 18, 19, 20, 21, 22, 23]. But there is little information about the interaction between laser sintered material and polymers. We can only infer their interaction from other tribological experiment carried out with iron (steel) and polymer [24, 25, 26, 27, 28, 29] or from an experiment performed with coated prototypes and polymer [30].
During the tribological experiments the most investigated properties are: friction coefficient, wearing rate, loading force, sliding velocity, temperature and surface properties.
Summarising what can be find in the literature it is established that the two big fields of the science (rapid prototyping and tribology) have been investigated together only a few times while the scientific support of the practice application would be needed.

2. Aim of the research work

The aims of our investigation were:

- To determine and to investigate the main parameters which have effect on CO_2 laser sintered specimen, and to make the model of the metal powder laser sintering;

6. I determined on the bases of "disk-on-cylinder type" tribological test investigation made at constant (1000 mm/s) sliding velocity between the laser sintered materials and the reinforced polyamide that: [S13-S16]

   increasing the normal loading force decreases the friction coefficient because of the adherence of the polyamide to the surface of the laser sintered material; modifying the polymer-metal contact to polymer-polymer contact;

   the degree of the reduction of the friction coefficient depends on the porosity of laser sintered material: the higher the porosity is the lower the friction coefficient becomes.

8. Publications

[S1] Takács J., Sklánitz A., Lovas A., Herczeg Sz.: Lézeres gyorsprototípus gyártás, 2. Ipari Lézer Alkalmazási Szeminárium, Balatonfüred, 2000. október 26-28., pp. 39-42, ISBN 963421554-8

[S2] Sz. Herczeg: Weiterentwicklung der Herstellungsbedingungen für das SLS Rapid Prototyping Verfahren, Neuartige Herstellungs- und Reparaturtechnologien in der Fahrzeugindustrie Kollokvium, Dresden, 20-22. 05. 2001, pp. 35-40, ISSN 1433-4135

[S3] Takács J., Herczeg Sz.: Gyors prototípusgyártás – növekvő versenyképesség, Gépgyártás XLI. évf. 7-8. szám, 2001. július-augusztus, pp. 11-18, ISSN 1587-4648

[S4] Takács J., Herczeg Sz.: A gyors és minőségi prototípusok előállításának jellemzői, Minőségügyi hírek XVI. évf., 2002. január, pp. 79-109, ISBN 1219-7602

[S5] Sz. Herczeg, J. Takács: Das klassische und das Laser-Sintern Methode, Neuartige Herstellungs- und Reparaturtechnologien in der Fahrzeugindustrie, Pardubice, 26-28. 05. 2002, pp. 55-64, ISBN 80-7194-449-1

[S6] Takács J., Herczeg Sz.: Gyors prototípusgyártás lehetőségei a járműgyártásban, 33. Autóbusz Szakértői Tanácskozás Nemzetközi Gépjárműbiztonsági Konferencia, 2002. szeptember 02-05., CD-ROM, 9. szekció: CAE módszerek a járműgyártásban, ISBN 963 9058 17 3

[S7] J. Takács, T. Markovits, Sz. Herczeg: The laser is a new tool in the manufacturing, Production processes and system, volume 1, Miskolc, 2002, pp. 151-159, HU ISSN 1215-0851

[S8] Herczeg Sz.: Gazdaságos, termelékeny módszerek, Magyar Műszaki Magazin II. évf. 1. szám, 2003. január-február, pp. 56-57, ISSN 1588-9300

[S9] Sz. Herczeg, J. Takács: Matching of subsystems rapid prototyping and optimisation of main process parameters, Materials, technologies, design, maintanance – their application in the field of transportation, Zilina, may 25-27, 2003, pp. 17-20, ISBN 80-8070-074-5

[S10] Sz. Herczeg, J. Takács: Matching of subsystems rapid prototyping and optimisation of main process parameters, Materials Engineering, Zilina (Szlovákia), 2003 Volume X, pp. 43-46, ISSN 1335-0803

[S11] Takács J., Herczeg Sz.: A gyors prototípusgyártás története és fejlesztési eredményei a lézertechnológiák bázisán, Gépgyártás XLIV. évf. 2004. 2-3. szám, pp. 4-8, HU ISSN 0016-8580

[S12] Sz. Herczeg, J. Takács: Influence of scanning speed on the mechanical and structural properties of laser sintered prototypes, Periodica Polytechnica Transport Engineering, Budapest. 2004 32/1-2, pp. 83-90, HU ISSN 0303-7800

[S13] Sz. Herczeg, J. Takács, L. Tóth, F. Franek, A. Pauschitz, T. Sebestyén: Tribological investigation of Fe-Ni-Cu based selective-laser-sintered rapid prototype tool models against fibre-reinforced polymer, Advanced Manufacturing and Repair Technologies in Vehicle Industry, Balatonfüred, may 17-19, 2004, pp. 174-178, ISBN 963 420 796 0

[S14] Sz. Herczeg, J. Takács, L. Tóth, F. Franek, A. Pauschitz, T. Sebestyén: The effect of sinter parameters on tribological properties of selective-laser-sintered rapid prototype tool elements, Proceedings 8th International Conference on Tribology, Veszprém, Hungary, jun 3-4, 2004, pp. 144-149

I optimised the laser scanning speed to ensure the highest relative shortening; [S12, S16]

4. On the bases of "disk-on-cylinder type" tribological test investigation between the laser sintered material and the reinforced polymer:
   I added to the present known "friction coefficient - friction distance" diagrams a new third section,
   and I described the properties of the three sections; [S13-S16, S20]

5. I determined after the tribological investigations made at constant (100N) loading force between the laser sintered materials and the reinforced polyamide that opposite to the published information the sliding velocity does not increase the friction coefficient in every case. Increased the friction velocity I established that the friction coefficient is sometimes increasing, sometimes decreasing and sometimes remain constant because of the porosity of the sintered samples: [S13-S16]

   In context of the investigated materials I determined that the friction coefficient:
   - is constant until glass transition temperature of the polyamide (in our investigation this was reached from the friction heat at 500 mm/s friction velocity),
   - is decreasing between the glass transition temperature and the long term service temperature of the polyamide (it was between 500 and 1000 mm/s friction velocity),
   - is suddenly increasing when the short term service temperature of the polyamide is reached (above 1000 mm/s friction velocity) and it will become stable in a smaller value;

   I determined that the higher the porosity is:
   - the higher the friction coefficient becomes until the glass transition temperature,
   - the lower the friction coefficient is between the glass transition temperature and the long term service temperature,
   - the more the friction coefficient increases next to the long term service temperature because of the embedding of the glass fibre parts in the pores of the sintered part. This effect is in proportion to the amount of the pores: the higher the number of the pores is the more polyamide gets embedded into them which increases the friction coefficient.

- to investigate the effect of the laser sintering parameters on the mechanical properties of specimens made from iron based power;
- to optimise the laser beam scanning speed to the mechanical properties (like: compression strength, relative shortening);
- to investigate the tribological interaction between the laser sintered material and a reinforced polymer:
  - to investigate the changing of the tribological phenomena depending on friction distance;
  - to investigate the tribolobical phenomena at different sliding velocity and at different loading force.

3. Materials, equipments and methods

3.1. Materials

The composition of the sintered powder, which is one of the typical metal powders used for selective laser sintering, is 72 Wt% iron, 20 Wt% nickel, 8Wt% phosphorous-bronze (containing 3,4% P). The grain diameter is Ø<50 μm. The size of the laser sintered model is Ø 10mm x 7mm (Fig 3.1.), the layer thickness is around 0.1 mm, the CO_2 laser power is around 150 W in continuous wave mode, the focused beam diameter on the surface is 0.2 mm and the scanning distance is 0.1 mm. The models are obtained with different scanning speeds of laser beam: 200, 300, 400, 500 and 600 mm/s.
The phosphorous-bronze grains constitute the component which has lower melting point. Iron and nickel are the components which melt at higher temperatures.

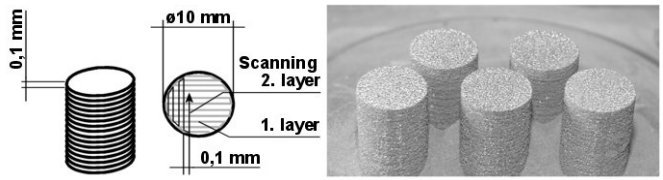

Figure 3.1.
The laser sintered specimens and their dimensions

The sintered specimens were worn by short fibre reinforced polyamide with 30% glass fibre content (Ertalon® 66-GF30) as counter body.
Before the tests the contact surface of sintered specimens was grinded (Ra ≈ 1,3 μm), and the cylindrical surface of the polymer counter bodies was turned. The diameter of counter bodies was between 35 and 40 mm, and the thickness was 3 mm.

3.2. Equipments of experiment

There are available laser sintering equipment for industrial application, but it was needed to develop a new equipment to control the processing during the laser sintering. The parameters of this developed equipment are variable between larger limits.
I developed and elaborated a Selective Laser Sintering laboratory equipment and technology at the Department of Vehicle Manufacturing and Repairing. It works on normal temperature using argon protective (figure 3.2.).

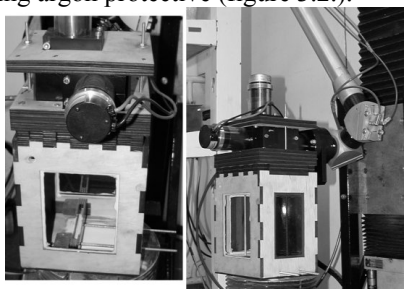

Figure 3.2.
The developed laser sintering equipment

The laser beam was moved in the "X-Y" plane with a special ("X" and "Y") mirror system activated by galvanic motors. All these were integrated into the scanning head. The scanning head and laser process was computer controlled. The possible maximum scanning speed was 10 m/s.
The moving laser mirrors have not cooling so the maximum of the laser power is 250W. The laser beam is focused by an f-Θ lens. The lens is made of Zn-Se, focus length is 200 mm and the working plan is 100x100 mm.
The position of the vertical ("Z") axes direction was actuated by stepping motor. This motor are controlled by a FRANKE SM2000 CNC controller with 0,01 mm accuracy.
In the closed working chamber it is possible to use different protective gas. The protective gas is circulated in the working camber ensured the cooling and the protection of the lens.

The tribological experiments were carried out in the Austrian Center of Competence for Tribology (AC^2T). Disk-on-cylinder test rig (Figure 3.3.) was selected for the tribological model investigation and the determination of the friction coefficient.
The sintered specimens were fixed and the counter bodies were rotating. The sliding velocity was changed by the speed of the rotating axis.
During the experiments the loading force, the friction force, the temperature on the surface of the sintered samples was measured and the friction coefficient was calculated. The temperature was measured at 1.5 mm wide from the polymer

I optimised the laser scanning speed compared to the tribological properties also. For the tribological investigations I used a polyamide polymer reinforced with 30% glass fibre.
Friction coefficient - friction distance diagrams between the sintered parts and the reinforced polyamide were measured. I determined the diagram can be divided into three characteristic sections, and I determined the topography of the specimens in these three sections.
In the available literature there is not any data about the friction coefficient between the laser sintered material and the reinforced polyamide for this I determined the friction coefficient belong to different sliding velocities and loading force.
The friction coefficient was measured at constant loading force at different sliding velocities using five different types of probes with different porosity produced by different laser scanning speed.
The friction coefficient was measured at constant sliding velocity also. And I determined the effect of porosity of the samples on the friction coefficient at different loading forces.
I described a new tribological phenomenon where the polymer was heated up by friction heat so much that its surface began to melt that the polymer and its glass fibre parts were embedded into the pores of the laser sintered specimens. The investigations were supported by metallography and SEM analysis.
It was possible to measure more accurately (compared to the commercial measuring method) the temperature of the contact surface, so I could determine the transformation point of the polyamide which caused the changes of the friction processes.

7. Summary of the new scientific results in thesis

1. I developed a CO_2 laser sintering test equipment by which it is possible to set the laser sintering parameters between wider limits than the apparatus available in the market are capable. I made its hardware and software integration. I tested it and I qualified its working according to the mechanical properties of sintered material. [S1, S2, S9-S12]

2. I systematised the acting factor for the one and more component metal powder laser sintering process. I selected which have determinate effect to the quality of the laser sintered part. [S5, S9-S12, S19]

3. I gave the limits of the laser scanning speed between them the laser sintering process is successful (at known conditions: P_{laser}, focused beam diameter, base material, etc.) and between this limits:
   I optimised the laser scanning speed to reach the highest compression strength; [S9-S12, S16]

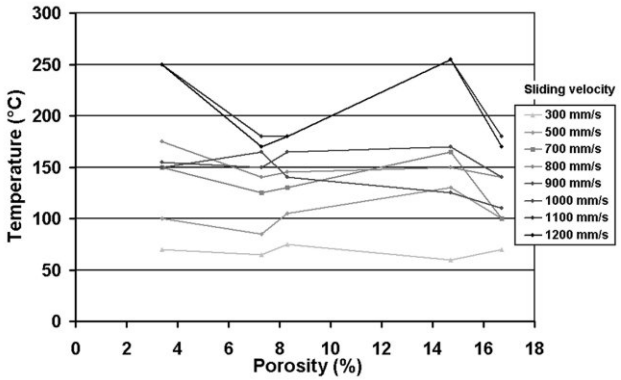

Figure 5.8.
The temperature depending on porosity and sliding velocity

Between 160 and 170°C it is achieved the sort term service temperature of PA 66-GF30. The strength of the polyamide is decreasing. The soft polymer and its glass fibre parts embed in to the pores of the laser sintered material. The friction coefficient is increasing. The worn surface of the laser sintered material will be bright and rough.
From the tribological experiments it is shown that the higher porosity increases the uncertainty of the friction coefficient and wearing. To take the mechanical strength of the sintered specimen and construction time into consideration the optimum of laser scanning speed is 400 mm/s.

6. Summary

In my investigation I elaborated the main process parameters of Selective Laser Sintering. These were systematised and the connections between of them were described. I selected which have a higher level of influence on laser sintering.
A Selective Laser Sintering laboratory equipment and technology was developed and elaborated in our institute. The parameters are variable between wide limits. We developed the software to the equipment as well.
The base material of laser sintering was a close mechanical mixture of 72 Wt% iron, 20 Wt% nickel and 8 Wt% phosphorous-bronze (containing 3 Wt% P) powders. I determined the laser sintering process parameters to CO_2 laser beam. I determined the limits of the laser beam scanning speed, and I optimised the scanning speed according to mechanical properties.
I determined the compression strength and the relative shortening of the sintered material made with different laser scanning speed, and I described the structures of the laser sintered materials at different scanning speed.

counter body. Frictional force was measured by strain gauges. The accuracy of the measurements in general was ± 5 %. The condition of the tests was dry friction at room temperature. The duration of test time of wearing process was usually 300 sec. Every measuring was repeated three times in all setting position.

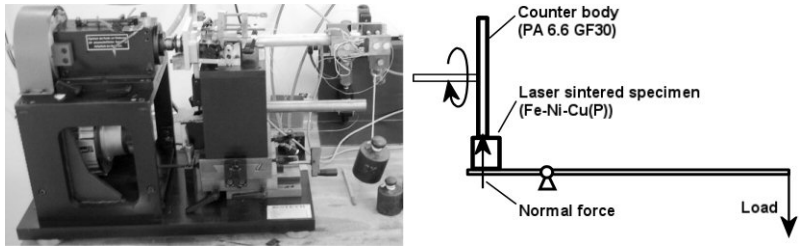

Figure 3.3.
The disk-on-cylinder test rig for the tribological investigation

3.3. Equipments of investigations

The laser-sintered probes were investigated by light microscope (ZEISS NEOPHOT 21). The compression ultimate strength was measured on INSTRON 1195. The roughness was measured with a RODENSTOCK RM600 laser topographer, MITUTOYO Surftest 301, HOMMEL TESTER T4000 surface roughness tester and NANOFOCUS µSurf® 3 dimensional surface topographer.
We investigated the worn surfaces using PHILIPS XL 40 scanning electron microscope. During the tribological investigation speed of the counter body was controlled by FUJI DIGITAL TACHO. The changing of the weight of the sintered samples was measured by SARTORIUS CP2245-0CE balance.
PHILIPS XL 30 electron microscope and JEOL JSM-840 electron-microprobe analyser was used to made pictures to analyse the composition of the metal powder in the laboratory of BME ATT. The powder's base material and the laser sintered specimens were investigated using a D8 ADVANCE (BRUKKER AXS) X-ray diffractometer in University of Miskolc Department of Physical Metallurgy and Metalforming.

4. Investigation of the laser sintered specimen

4.1. Process parameters of laser sintering

The interactions during laser cutting, laser welding and laser brazing were already summarised. At more component metal powder laser sintering it was missing.
At first I collected the acting factors of other laser added processes (laser cutting, welding, brazing). I investigated which have had effect on the laser sintering process also. I grouped them and they were completed after my experimental work.
I selected which have determinate effect to the quality of the laser sintered part. These are the input data.

Their connection system is shown on figure 4.1. During the experiments one component was changed and the others were constant (it was made parametric experiment).

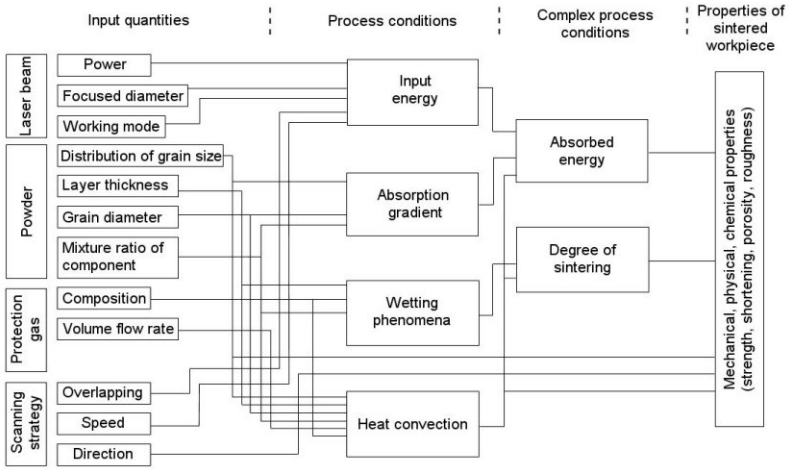

Figure 4.1.
The simplified model of laser sintering

4.2. The effects and the limits of the laser scanning speed

The moving speed of the laser beam has a great effect on the absorbed energy that is why needed to investigate the effect of the laser scanning speed.
The scanning speed of laser beam was changed with step of 100 mm/s. We determined the border of scanning speed at Selective Laser Sintering Process for Fe-Ni-Cu alloy powder. If scanning speed is less than 200 mm/s the investigated metal powder will be melted if greater than 600 mm/s then the sintering will not be taken place (figure 4.2.).
If the laser scanning speed is less than 200 mm/s, metal powder would be melted. The melted grains are formed irregular shape after the solidification caused by surface-tension. This inhibits the sintering process because the following layer is not possible to make (for example in 0.1 mm thick). If the laser scanning speed is over 600 mm/s, the metal powder will not be sintered.
Between the limits of the laser scanning speed five different types of laser sintered specimens were made namely with 200, 300, 400, 500 and 600 mm/s of laser scanning speed. The porosity of the specimens made with different scanning speed was summarised in table 4.1. The differences between the values of the porosities are caused by the melting process of the components in the metal powder and by the different absorbed energy at the different laser scanning speed. These phenomena need additional investigations.

5.4. Investigation of temperature during the wearing processes

Properties of polymers are changing in small interval of temperature. Measuring the temperature of contact surface is not possible. That is why the ambient temperature is given at the tribological investigations.

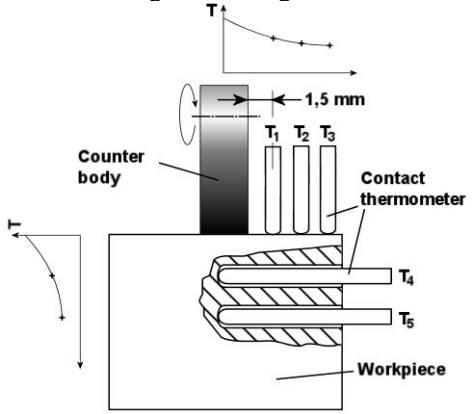

Figure 5.7.
Calculating the temperature using contact thermometer

The temperature distribution is not homogeneous on the contact surface but during my investigation I assumed nearly homogeneous distribution on an average temperature. A temperature measuring system was build from five contact thermometer to calculate the temperature on the contact surface. So it was possible to calculate the temperature more precise. This system is shown on figure 5.7.
The temperature depending on porosity and sliding velocity is shown on figure 5.8. During the investigations the maximum of temperature was 240-260°C. It means that it was enough to investigate the changes only on polyamide 66-GF30.
At lower sliding velocity the temperature was between 50 and 100°C. The glass transition temperature of PA 66-GF30 is between these values also [31, 32, 33, 34]. According to the tribological investigation the friction coefficient is nearly constant. In this area the worn surface of the sintered specimen are mat and smooth the surface roughness of the specimen is decreasing.
Above the glass transition temperature (100-150°C) the polyamide becomes softer, on the surface of laser sintered metal there will be a thick polyamide layer, the friction coefficient is decreasing, the surface roughness is nearly constant. In this temperature area is the long term service temperature of PA 66-GF30 [31, 32, 33, 34].

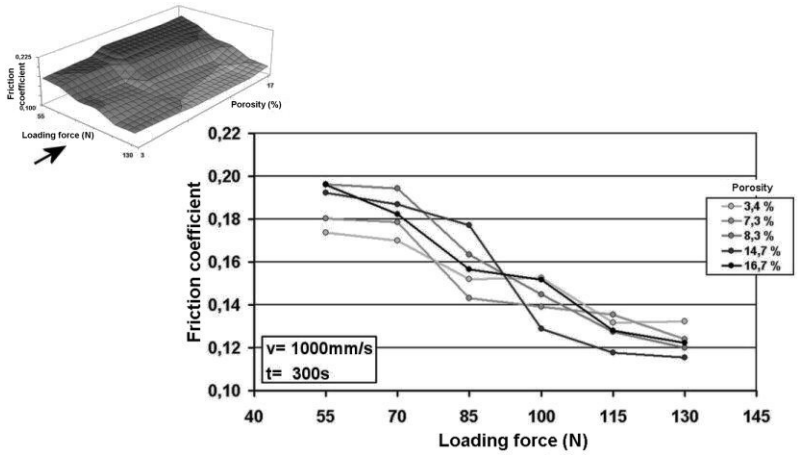

Figure 5.5.

Friction coefficient depending on loading force at constant sliding velocity

At lower loading force (55-70 N on figure 5.6.) friction coefficient increases because of changing of the surface roughness. At higher loading force (100 - 130 N on figure 5.6.) the porosity does not increase but decreases the friction coefficient because the reasons in the 5.2. chapter mentioned.

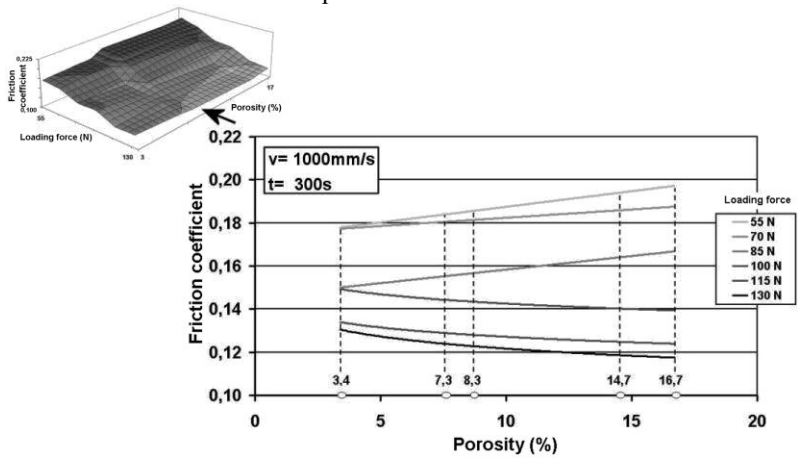

Figure 5.6.

Friction coefficient depending on porosity at constant sliding velocity

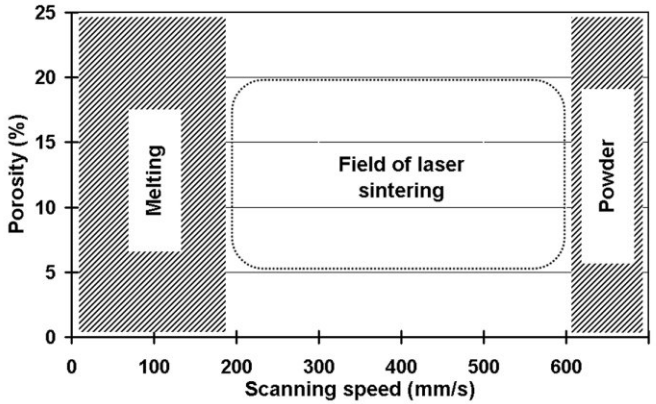

Figure 4.2.

The limits of the laser sintering using Fe-Ni-Cu(P) metal powder

Because we could made many specimens with different laser scanning speed it was possible to optimise the laser scanning speed. It was optimised according to the mechanical properties like ultimate compression strength and relative shortening.

Table 4.1.

The porosity of the specimens

Scanning speed (mm/s)	Porosity (%)	Scattering
200	3,4	± 1,17
300	16,7	± 2,89
400	7,3	± 1,20
500	14,7	± 2,64
600	8,3	± 2,26

In the available literature only the ultimate tensile strength was given [5, 14] so we investigated the ultimate compression strength of the specimens.

On figure 4.3. the ultimate compression strength of the specimens is shown. The differences between the ultimate compression strength of the specimens made with different laser scanning speed are caused by the processes during the laser sintering process. These processes are different from the processes during the commercial sintering process so it was needed to investigate their background.

The texture of the powder's base material and the laser sintered specimens processed using different scanning speeds were investigated using an X-ray diffractometer. The results of the measuring are shown on figure 4.4.

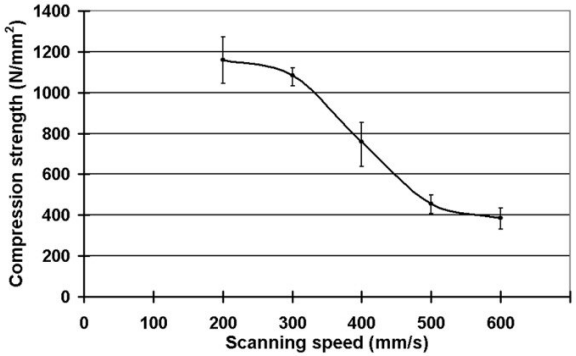

Figure 4.3.

The ultimate compression strength of the specimens made with different laser scanning speed

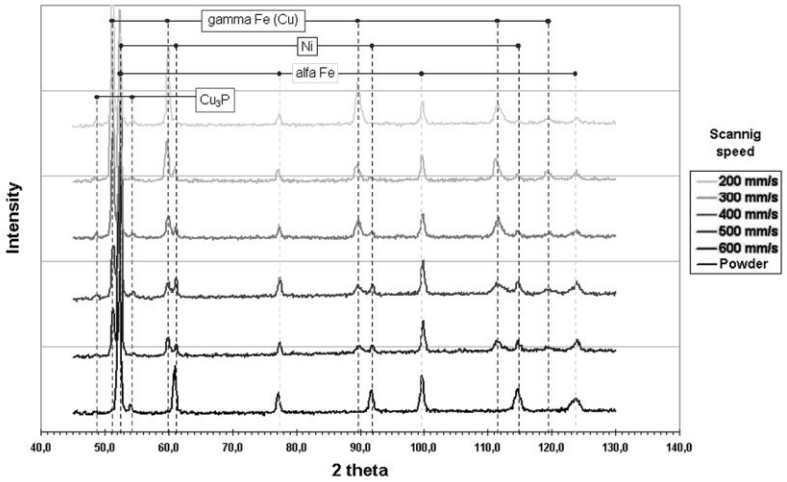

Figure 4.4.

X-ray diagram of the laser sintered specimens made by different scanning speed

As I mentioned the composition of the sintered powder is 72 Wt% iron, 20 Wt% nickel, 8Wt% phosphorous-bronze (containing 3,4% P). According to the composition there are four phases in the base material, these starting phases in the powder are shown on the X-ray diagram: alpha ferrite, nickel, copper and copper-phosphide (Cu_3P).

The base material was heated by moving laser beam. The lower moving speed (scanning speed) means higher absorbed energy. It is shown on the diffractograms that increasing the absorbed energy the degree of the sintering process will be higher.

At middle sliding velocity (700-900 mm/s), the polymer counter body is heated up by friction heat and the softer polymer has a lower friction coefficient. Due to the higher velocity, the sharp edges of the pores brake off and the friction coefficient decreases.

At higher sliding velocity (1000 - 1200 mm/s) the friction coefficient decreases caused by sliding velocity. But a new phenomenon is that the porosity does not decrease the friction coefficient but the porosity increases it (area 'G' on figure 5.3.) Over 1000 mm/s the counter body will be warmed up so much that its surface begin to melt, then the polymer and the broken glass fibre parts will be embedded into the pores (figure 5.4.) which results in the increase the friction coefficient (area ‘F’ on figure 5.3.).

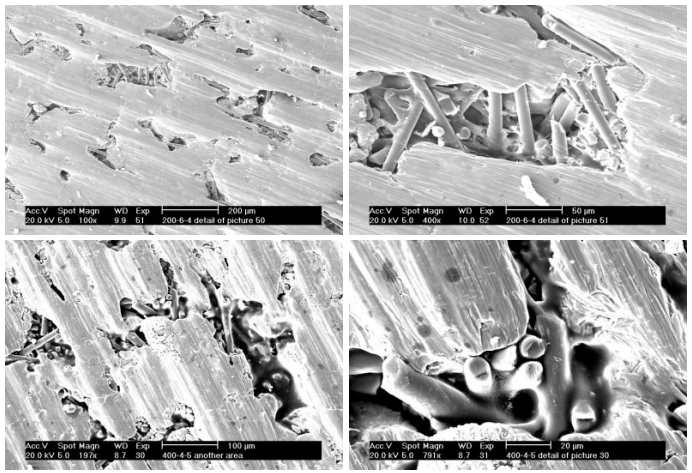

Figure 5.4.

The polymer and the glass fibre parts embedded in the pores of the sintered part

5.3. Friction coefficient depending on loading force

During the investigation the sliding velocity we choose constant 1000 mm/s. The loading forces were 55, 70, 85, 100, 115 and 130 N. The result of the measuring is shown of on figure 5.5. From the measured values of friction coefficient an other diagram of friction coefficient and porosity was drawn (figure 5.6.).

The increase of normal load causes the decrease of friction coefficient between Fe-Ni-Cu(P) and PA 66-GF30, it is similar to the published information.

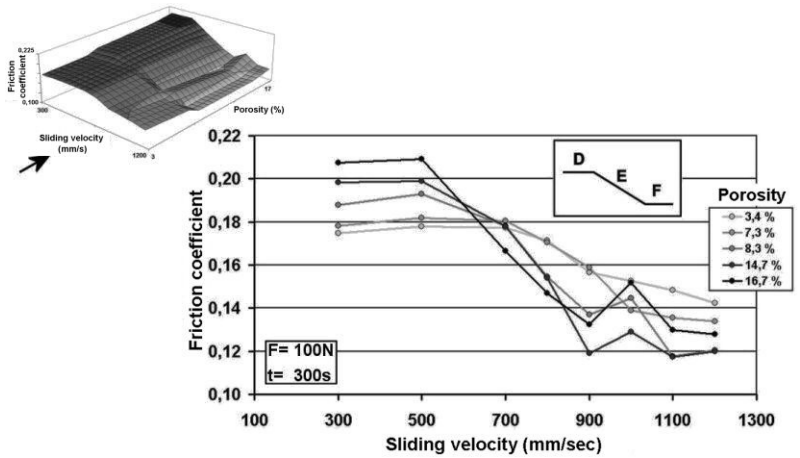

Figure 5.2.

Friction coefficient – Sliding velocity diagram for various porosity

Figure 5.3. shows if porosity raises, then at low sliding velocity (300-500 mm/s) friction coefficient increases. The increase of porosity results the increase of surface roughness because the wearing of the specimens is not significant [31]. The soft polyamide increases the deformation force at higher surface roughness so the friction coefficient increases also.

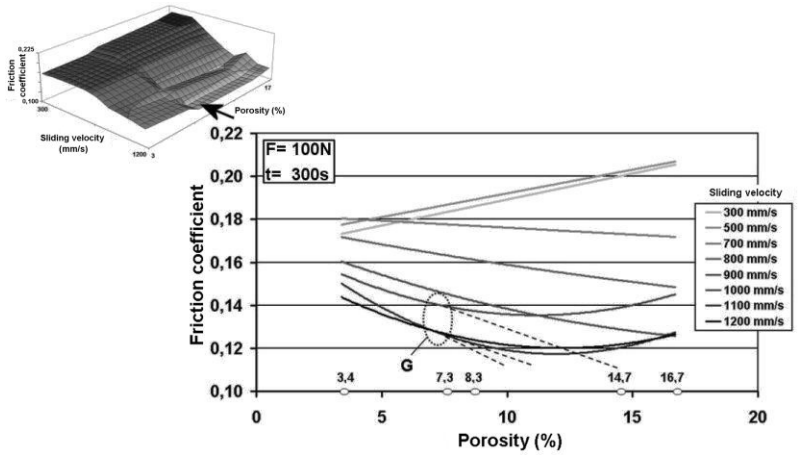

Figure 5.3.

Friction coefficient depending on porosity at constant loading force

Using selective laser sintering the order of melting is determined not only by the components but also by the absorption capability of the materials. If the absorption degree is higher, the grains warm up faster and they may melt earlier. Equilibrium phases do not come into existence during the laser sintering process because of the limits of the inhomogeneous temperature distribution and the time.

On figure 4.4 is shown that after the sintering process the amount of α-Fe and Ni phases decreases and they constitute a new (fourth) phase. From the calculated lattice parameter it is verifiable that the fourth phase is a cubic face-centred latticed phase. The amount of the Cu_3P phase decreases also. This phase occurs by diffusion of nickel into the iron which is in γ-phase on the temperature of laser sintering. During the cooling period the part of γ iron which does not contain enough nickel changes into alpha ferrite. It can also be pointed out from the differences of the ferrite's and nickel's lattice parameters. During the cooling the part of the γ-iron which contains relatively higher nickel remains unchanged as γ-phase.

The amount of the Cu_3P phase decreases also but well-determined tendency can not be demonstrated because of the small amounts. If Cu_3P phase breaks down the copper phase is not able to distinguish from the γ-phase because their lattice parameters are close to each other (3,597 and 3,6 Å). So the γ-phase and the Cu are shown together on the figure 4.4.

At a given material not only the value of the compression strength is important but the ultimate relative shortening also. These are important at computer aided simulation of a workpiece made from this material. So I measured the ultimate relative shortening of the laser sintered materials made with different laser scanning speed. The results of the experiments are shown on figure 4.5.

Because of the above mentioned phase conditions even more material comes to being which has a higher relative shortening.

From the diagrams I established that higher mechanical strength is at lower laser scanning speed. The optimal laser scanning speed is 300 mm/s according to the mechanical strength and the construction time.

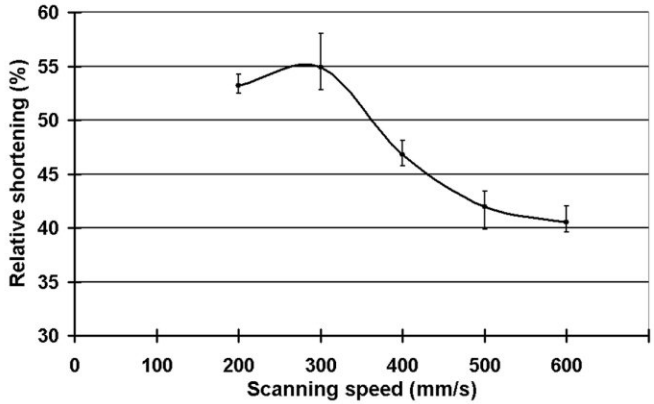

Figure 4.5.
The relative shortening of the specimens made with different laser scanning speed

5. Tribological investigations

5.1. Sliding distance dependence of friction coefficient

In the available literature there is not any data about the tribological properties of the laser sintered materials so we investigated them. In first step the friction coefficient depending on distance was determined.

To the tribological investigation laser sintered Fe-Ni-Cu(P) and glass fibre reinforced polyamide PA 66 GF30 was used, the loading forces were 55, 70, 85, 100, 115 and 130 N, the values of sliding velocity were 300, 500, 700, 800, 900, 1000, 1100 and 1200 mm/s.

During the investigations the characteristic of the diagrams was always similar. One of the typical diagrams is shown on figure 5.1.

In the literature is published that these diagrams can be divided in to two characteristic sections. The first ('A') is an increasing section, the second ('B') is a constant section. I determined that at the investigated two materials a new third section can be added to the diagram after section 'B'. The third section is an instable increasing section.

To investigate the wearing phenomena we measured before and after the testing the surface roughness (Ra) on the machined sintered part ($R_{a\ sinter\ A}$ = 1.32 µm) and on the counter body ($R_{a\ counter\ A}$ = 1.59 µm). In the first part of the diagram (area 'A') friction coefficient is increasing because the contact surface are changing from a line contact to a surface contact and according to them surface specific loading is decreasing. The measured average surface roughness of the sintered part decreases until $R_{a\ sinter\ B}$ = 0.52 µm and the counter body until $R_{a\ counter\ B}$ = 0.68 µm. In a few seconds there will be a constant condition of wearing process (area 'B') and in this area the friction coefficient fluctuates in a smaller interval. There will be a point

where the friction coefficient will increase again (area 'C'). The polymer component of the counter body on the contact surface wears out and the glass fibres remain on the surface changing the characteristics of the wearing process. The polymer and the broken glass fibre parts fill up the pores of the sintered specimen increasing the friction coefficient. The average surface roughness of the sintered part increases until $R_{a\ sinter\ C}$ = 4.92 µm.

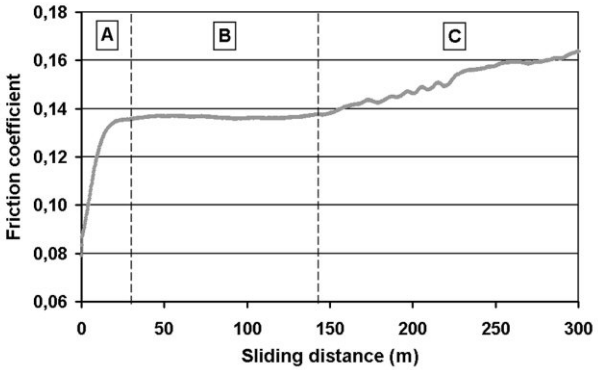

Figure 5.1.
The sliding distance dependence of friction coefficient

5.2. Friction coefficient depending on sliding velocity

During the investigation the loading force was constant 100 N and the friction coefficient was measured at different sliding velocities (300, 500, 700, 800, 900, 1000, 1100 and 1200 mm/s) using five different types of probes with different porosity produced by different laser scanning speed. The value of porosity is: 3,4%; 7,3%; 8,3%; 14,7%; 16,7%.

From the measured value of friction coefficient a Sliding velocity – Friction coefficient diagram was drawn (Figure 5.2.). From the diagrams we determined that they could be divided into three sections (D, E, F).

At lower porosity if the sliding velocity is increasing then the friction coefficient decreasing (see figure 5.2.) because the higher velocity decreases the adhesion between the laser sintered material and the polyamide. It is similar to the published information between solid metal and polymer [28]. It means that lower porosity has not significant effect on the friction coefficient at the investigated materials.

From the values of friction coefficient, which are shown on figure 5.2., a friction coefficient and porosity diagram was drawn (see figure 5.3.).